Xiaokun Man[1], Lijun Jin[1*], Guang Xu[2], Zihan Yu[3], Fucheng Wu[3] Yingye Zhu[3]

J. Electrical Systems 18-3 (2022): 304-317

Regular paper

Multi-objective comprehensive optimization based on probabilistic power flow calculation of distribution network

In recent years, distributed generation technology develops rapidly due to its' flexible and environment-friendly nature, and the wide application of electric vehicles poses a challenge to the safety of the system. In order to better analyze the impact of DG on the economics and safety of distribution networks, a probability model for random load, micro gas turbines and photovoltaic power generation system is formulated. With the objective of minimizing the network loss, lowest static insecurity probability, and the lowest cost of purchasing electricity, the optimization of distribution network with distributed generation is carried out by adjusting the distribution network topology and the output of controllable DG. The stochastic power flow is combined with the particle swarm optimization algorithm to obtain the Pareto non-inferior solution set, and then the subject is selected to obtain the optimal solution. Finally, simulations are carried out on the IEEE 33-bus test system and it is shown that the proposed method can effectively reduce the network loss and static insecurity probability on the basis of low cost of purchasing electricity.

Keywords: Distribution network; Stochastic power flow; Electric vehicles; Static probability of insecurity; Multi-objective comprehensive optimization

1. Introduction

As the proportion of electric vehicles [1] in urban power grids gradually increases, the mode of bidirectional energy transmission [2] of electric vehicles in the power grid will gradually develop in the urban power grid [3-4]. At the V2G mode, the charge and discharge characteristics of electric vehicles will be affected by many aspects, such as the type and charge and discharge mode of electric vehicles, the driving law of users, the scale of the development of electric vehicles, and so on, which leads to the great uncertainty of the charge and discharge power of electric vehicles. These uncertain factors will pose a great challenge to the safety of the power grid during the large-scale grid connection of electric vehicles, so it is of great significance to analyze the randomness of charge and discharge power of electric vehicles reasonably.

Distribution network reconfiguration (DNR) [5-6] is to optimize the distribution network operation by combining the state of the distribution switch according to the load of the distribution network and the output power of the distributed generation (DG). The advantages of distributed power supply, such as flexibility, economy and environment-friendliness, make it widely used in distribution network to reduce distribution network loss and improve node voltage.

* Corresponding author: Lijun Jin, College of Electronic and Information Engineering,Tongji University, Shanghai 201804, China, E-mail: jinlj@tongji.edu.cn
[1] College of Electronic and Information Engineering, Tongji University, Shanghai 201804, China.
[2] Zhuhai Xujizhi Power Automation Co., Ltd, Zhuhai, 519060, China
[3] College of Electrical Engineering and Automation, Shandong University of Science and Technology, Qingdao 266590, China.

The output of DG is generally regarded as a fixed value in the research of distribution network reconfiguration [7]. With the increasing proportion of distributed power supply into power grid, the influence of uncertain factors on the operation of distribution network becomes more and more obvious. In order to make the research of distribution network more practical, it is more and more important to deal with the uncertain factors reasonably [8-11]. In [10], scene partition method based on Wasserstein distance index is used to solve the DNR problem. The wind power output and the load are divided into scenarios, and the strategy of the optimal scheme is determined by comparing the schemes of different scenarios. This method is one-sided in the consideration of uncertainty, and the result is limited, and the probability distribution of the output of state variables cannot be obtained. In [11], distribution network reconfiguration is studied considering the randomness of load and wind power generation, and two-point estimation method is used to calculate stochastic power flow. The probability distribution of output can be obtained by calculating the deterministic power flow 2*n* times each time (*n* is the number of injected random variables), but when applied to the reconfiguration problem, too many power flow calculations make the calculation time of DNR very long. The practicability of this method is poor for the large-scale distribution system.

There are few optimization studies considering the randomness of electric vehicles, and all these methods obtain the operation state of distribution system by deterministic power flow which is time-consuming. Considering the above shortcomings, this paper establishes the stochastic probability model of electric vehicle, photovoltaic, gas turbine and load, taking network loss, static unsafe probability and power purchase cost as objective functions [12 -14], and the optimal solution set can be obtained by using the Pareto criterion [15] to deal with the multi-objective optimization problems. Finally, the optimal solution can be obtained according to the preference of the decision maker, so as to improve the static security and economy of the distribution system.

2. Notation

The notation used throughout the paper is stated below.

λ_i	Probability of node *i* voltage exceeding the limit
U_i	voltage of node *i*
$U_{i\max} / U_{i\min}$	Upper and lower limits of the node voltage
$\Pr\{\}$	probability of the inequality
n	number of nodes in the system
f_1	active power loss of the distribution network
r_i	resistance of the line i
P_i / Q_i	active and reactive power flowing through the end terminal of line *i*
T	branch set of the distribution network
s_1	price of purchasing electricity from gas turbine
$P_a /$	active power output of gas turbine
s_2	purchase price of the main network
P_c	active power output of the main grid system to the system
c_1	node set of gas turbine output

g_k	current network topology
G_k	the set of network topology that satisfies connectivity and radiality
$S_{i,\max}$	maximum power limit of branch i
$P_{G,k}$ / $Q_{G,k}$	active and reactive power output of the controllable DG k
$P_{G,k,\max}$ / $Q_{G,k,\max}$	maximum active and reactive power that controllable DG k can output
d	the daily journey of an electric vehicle
t_s	electric vehicles day start time
t_e	day-end time for electric vehicles
r	actual and maximum values of light intensity during this time period
p	normal operating probability of the gas turbine
C	rated power of the gas turbine
w	actual power generation of the gas turbine
S	injection power of the node
X	variable expressed by the node state quantity
g_υ	normalized value of the semi-invariant υ-order
$\overline{x}$	normalized randomly variables
$H_\gamma(x)$	Hermitian polynomial
p_{id} / p_{gd}	individual and global optimal particle positions
x_{id} / v_{id}	particle position and velocity
t / $t_{\max}$	current and maximum iteration number of iterations
ω	inertia constant
D	number of objective functions
$g(x)$ / $h(x)$	equality and inequality constraints
$F(k)$	magnitude of the evaluation value of the k-th solution
α / β	parameters of the Beta distribution
$\omega_{\min}$ / $\omega_{\max}$	minimum and maximum inertia constant
a / b / c	decision factors
s_1	price of purchasing electricity from gas turbine [k$/MW]
s_2	purchase price of the main network [k$/MW]

3. Multi-objective comprehensive optimization model

3.1. Objective function

(1) System static security

In this paper, the probability of voltage violation is taken as the static security index of the system. The probability λ_i that the node i voltage exceeds the limit can be expressed as

$$\lambda_i = \Pr\{U_i > U_{i\max}\} + \Pr\{U_i < U_{i\min}\} \tag{1}$$

The probability of voltage not exceeding the limit is 1-λ_i, and the probability of voltage exceeding the limit of the whole system is as follows

$$\lambda = 1 - \prod_{i=1}^{n}(1-\lambda_i) \tag{2}$$

(2) Economy of system operation

The network active power loss and the power purchase cost per unit time (1h) are taken as the evaluation indexes of the operation economy of the system.

The optimization objective of active power loss is expressed as follows

$$\min f_1 = \sum_{i \in T} r_i \frac{P_i^2 + Q_i^2}{U_i^2} \tag{3}$$

For the distribution system with distributed generation, the cost of purchasing electricity per unit time is closely related to the output of the distributed power supply. The optimization target of the purchase cost can be expressed as follows

$$\min f_2 = \sum_{a \in C_1} s_1 \times P_a + s_2 \times P_c \tag{4}$$

3.2 Constraints

Comprehensive optimization of distribution network needs to meet the following constraints

(1) The distribution network is radial and there are no isolated nodes in it, which means there is no loop and no islands.

$$g_k \in G_k \tag{5}$$

(2) Voltage constraint

$$U_{i\min} \le U_i \le U_{i\max} \tag{6}$$

(3) Branch capacity constraint

$$\sqrt{P_i^2 + Q_i^2} \le S_{i,\max} \tag{7}$$

(4) Constraint of DG output

$$\begin{cases} P_{G,k} \le P_{G,k,\max} \\ Q_{G,k} \le Q_{G,k,\max} \end{cases} \tag{8}$$

3.4 Probability model of DG and load

(1) Model of photovoltaic power generation

The distribution of light intensity roughly satisfies the Beta distribution, and its probability density function is

$$f(r) = \frac{r(\alpha+\beta)}{r(\alpha)r(\beta)} \left(\frac{r}{r_{\max}} \right)^{\alpha-1} \left(1 - \frac{r}{r_{\max}} \right)^{\beta-1} \tag{9}$$

α and β can be determined by the expectation and variance of the light intensity

$$\alpha = \mu \left[\frac{\mu(1-\mu)}{\sigma^2} - 1 \right] \tag{10}$$

$$\beta = (1-\mu)\left[\frac{\mu(1-\mu)}{\sigma^2} - 1\right] \tag{11}$$

The power generated by the photovoltaic array is

$$P_M = rA\eta \tag{12}$$

where A represents the total area of the battery panel, and η represents the photoelectric conversion efficiency.

It is known from equation (12) that when the illumination intensity satisfies the Beta distribution, the power generated by the photovoltaic array also satisfies the Beta distribution

$$f(P_M) = \frac{\Gamma(\alpha+\beta)}{\Gamma(\alpha)\Gamma(\beta)}\left(\frac{P_M}{R_M}\right)^{\alpha-1}\left(1-\frac{P_M}{R_M}\right)^{\beta-1} \tag{13}$$

(2) Model of micro-gas turbine

Synchronous generators and DG controlled by voltage-type inverters can be regarded as PV nodes. In the iterative process of power flow calculation, they can be converted into PQ nodes for processing.

In this paper, the two states (normal operating state and fault outage state) probabilistic models are used to represent the operating state of the gas turbine

$$P(W = w_i) = \begin{cases} p & w = C \\ 1-p & w = 0 \end{cases} \tag{14}$$

We assume that the gas turbine input power meets the binomial distribution. It is assumed that the input power of gas turbine satisfies the binomial distribution in this paper.

(3) Load model

Operational practices have shown that the uncertainty of distribution load can be approximately reflected by a normal distribution. Thus, the probability distribution of active and reactive loads can be expressed as

$$f(P) = \frac{1}{\sqrt{2\pi}\sigma_P}\exp\left(-\frac{(P-\mu_P)^2}{2\sigma_P^2}\right) \tag{15}$$

$$f(Q) = \frac{1}{\sqrt{2\pi}\sigma_Q}\exp\left(-\frac{(Q-\mu_Q)^2}{2\sigma_Q^2}\right) \tag{16}$$

4. Probabilistic power flow

The existing probabilistic power flow algorithms can be roughly divided into three categories: analytical method, simulation method and approximation method. In this paper, the analytic method is used to calculate the probabilistic power flow. Based on the DC power flow equation and the linearized AC power flow equation, it is considered that there is no correlation between the random distribution of injection power. The probability distribution function of injection power is obtained according to convolution calculation,

and then the probability distribution of node voltage is calculated according to the linearized power flow equation.

4.1 Power flow equation linearization

In power flow calculation, the node power equation can be represented by $S=f(X)$. In stochastic power flow calculation, random variables can be expressed by their expected values and random perturbation values obeying a certain distribution.

$$S = S_0 + \Delta S \tag{17}$$

$$X = X_0 + \Delta X \tag{18}$$

The Taylor series expansion of (20) is

$$S_0 + \Delta S = f\left(X_0 + \Delta X\right) = f\left(X_0\right) + J_0 \Delta X + \ldots \tag{19}$$

where $S_0=f(X_0)$. If ignoring the high order derivatives, we get

$$\Delta X = J_0^{-1} \Delta S \tag{20}$$

Where X_0 is solved by deterministic power flow, J_0 is the Jacobian matrix used in the last power flow calculation, that is, sensitivity matrix. Equation (23) is a linearized nodal power equation. By convolution calculation, the probability distribution of output random variable ΔX can be obtained from the distribution of injected power ΔS.

4.2 Process of probabilistic power flow

The proposed probabilistic power flow algorithm consists of seven major steps which are described as follows:

Step1. Enter the original data. Including the data needed for general power flow calculation and the related data of random variables, such as those satisfying normal distribution, the variance and expectation values should be given.

Step2. The expectation and variance of light intensity distribution are obtained from the measured value of light intensity distribution in a certain time range (such as a day or a month). According to equation (15), the initial value of output of photovoltaic power generation system is obtained.

Step3. The deterministic power flow calculation is carried out, and the expectation of node voltage U and Jacobian matrix J_0 are calculated under the reference operation state, and the sensitivity matrix S_0 is obtained.

Step4. The moment of each order is obtained from the probability distribution function of random variable, and the semi-invariant of each random variable is obtained according to the relation between moment and semi-invariant.

Step5. The calculated semi-invariants are added according to their properties, that is $\Delta S^{(k)}=\Delta S_l^{(k)}+\Delta S_G^{(k)}+\Delta S_P^{(k)}$, where $\Delta S_l^{(k)}$, $\Delta S_G^{(k)}$, and $\Delta S_P^{(k)}$ denotes k-order semi-invariants of load power, injection power for gas turbine and photovoltaic power generation systems, from which the semi-invariants of injection power for each node are obtained.

Step6. According to equation (20), the semi-invariants $\Delta S^{(k)}$of the injection power of each node obtained from the previous step are calculated to obtain the semi-invariants $\Delta X^{(k)}$ of each order of the state variable.

Step7. The cumulative distribution and probability density function of the state variable ΔX are obtained by using the formula of the expansion of the Gram-Charlier series [17]. The expression is as follows

$$f(x)=\varphi(\bar{x})[1+\frac{g_3}{3!}H_3(\bar{x})+\frac{g_4}{4!}H_4(\bar{x})+\frac{g_5}{5!}H_5(\bar{x})+\frac{g_6+10g_3^2}{6!}H_6(\bar{x})+\frac{g_7+35g_3g_4}{7!}H_7(\bar{x})+\frac{g_8+56g_3g_5+35g_4^2}{8!}H_8(\bar{x})+\cdots] \tag{21}$$

$$F(x)=\phi(\bar{x})+\varphi(\bar{x})[\frac{g_3}{3!}H_2(\bar{x})+\frac{g_4}{4!}H_3(\bar{x})+\frac{g_5}{5!}H_4(\bar{x})+\frac{g_6+10g_3^2}{6!}H_5(\bar{x})+\frac{g_7+35g_3g_4}{7!}H_6(\bar{x})+\frac{g_8+56g_3g_5+35g_4^2}{8!}H_7(\bar{x})+\cdots] \tag{22}$$

$H_\gamma(x)$ is the coefficient after finding the derivative of order γ for$\phi(\bar{x})$.

Step8. The state variables and the confidence interval of branch power flow can be calculated by using the obtained cumulative distribution function. Calculating of voltage out-of-limit probability of the entire distribution system according to formula (2).

5. Implementation of optimization algorithm

5.1 Particle swarm optimization

In order to enhance the optimization ability, the PSO iterative process is dynamically optimized. The ω is used to maintain the original flight velocity of the particle, and its dynamic improvement is made to expand the search space when the particle is flying to the optimal position and avoid being restricted to the local region. The dynamic learning factor can continuously balance the global and local search capabilities, making it have a strong cognitive ability in the early iteration, and enhance the social learning ability of the particles in the later iteration.

$$v_{id}=\omega * v_{id}+c_1r_1(p_{id}-x_{id})+c_2r_2(p_{gd}-x_{id}) \tag{23}$$

$$x_{id}=x_{id}+v_{id} \tag{24}$$

$$\omega=\omega_{\min}+((\omega_{\max}-\omega_{\min})\times(t_{\max}-t))/t_{\max} \tag{25}$$

$$c_1=c_{1a}+\frac{c_{1b}-c_{1a}}{t_{\max}}\times t \tag{26}$$

$$c_2=c_{2a}+\frac{c_{2b}-c_{2a}}{t_{\max}}\times t \tag{27}$$

5.2 Multi-objective optimization

The mathematical model of the Pareto multi-objective optimization method can be expressed as

$$\begin{cases} \min F(x) = \left[f_1(x), f_2(x), \cdots, f_D(x) \right] \\ s.t \qquad g(x) = 0, h(x) \le 0 \end{cases} \tag{28}$$

The optimal solution can be obtained from the dominating relationship of the solution. The optimal solution is often a solution set composed of multiple solutions. The decision maker can choose the appropriate solution from the optimal solution set according to his own bias. In this paper, the selection strategy is used for individual selection. *a, b,* and *c* are the decision factors, and their size can be determined by the decision makers, reflecting the proportion of each objective function in the evaluation value.

$$\begin{cases} F(k) = a \times \dfrac{f_1(k) - f_{1\min}}{f_{1\max} - f_{1\min}} + b \times \dfrac{f_2(k) - f_{2\min}}{f_{2\max} - f_{2\min}} + c \times \dfrac{f_3(k) - f_{3\min}}{f_{3\max} - f_{3\min}}, \\ \text{s.t} \qquad \text{a+b+c} = 1 \end{cases} \tag{29}$$

where $f_1(k)$, $f_2(k)$ and $f_3(k)$ respectively represent the fitness values of the three objective functions of the kth solution. $f_{1\max}$, $f_{2\max}$ and $f_{3\max}$ respectively represents the maximum fitness value of the three objective functions in the solution set. $f_{1\min}$, $f_{2\min}$ and $f_{3\min}$ respectively represent the minimum fitness values of the three objective functions in the solution set, that is, the optimal values. By comparing the magnitude of the evaluation value, the priority level of the solution can be determined, and the final optimal solution can be determined for the decision maker.

5.3 Algorithm flowchart

A flow chart of the comprehensive optimization algorithm based on stochastic power flow is shown in Figure 1.

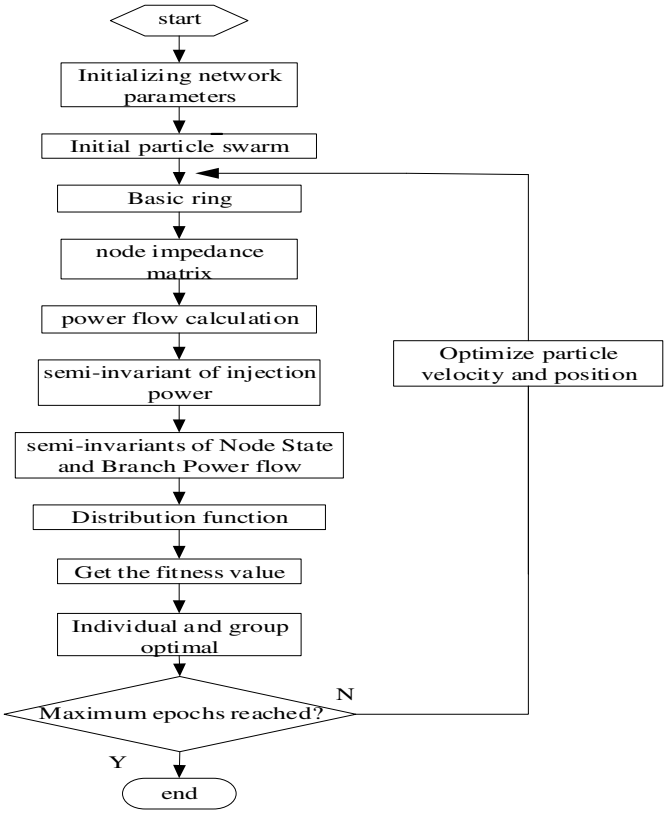

Figure 1**.** Flow chart of the Comprehensive optimization

6. Case study

The effectiveness of this algorithm is verified by the PG&E 69 bus system [17]. The system consists of 69 nodes ,73 branches and 5 contact switches. Set the benchmark parameter as U_b= 12.66kV and S_b =1MVA.

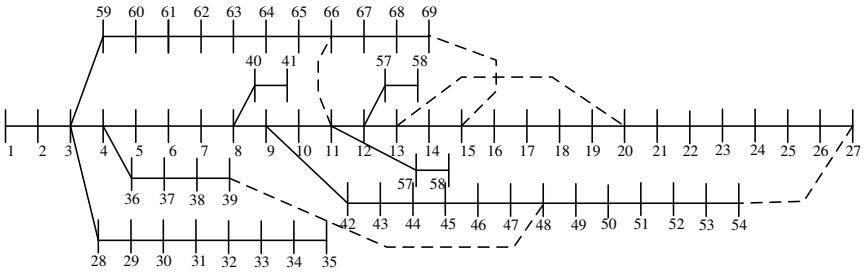

Figure 2. PG&E69 bus system

An electric vehicle charging station is connected to node 5 and 12, and the expected value of active power and reactive power absorbed from the power grid is 400 kW and 8kW respectively, with 10% of the expected value of variance. Join the photovoltaic power generation system at nodes 32 and 66, the two parameters of the light intensity are both 0.9,

and the upper limit of the output power is 400kW. Adding micro gas turbines (controllable DG) at nodes 20 and 47, the upper limit of active power output is 300kW, the power factor is 0.9, and the availability rate is 0.9. The original load data is taken as its expected value, and the standard deviation is 30% of the expected value.

6.1 Analysis of power flow results

In order to verify the correctness of the semi-invariant stochastic power flow algorithm, it is compared with the Monte Carlo simulation method, in which the number of sampling of the Monte Carlo simulation method is 6000 times. Suppose the network topology is the original structure, and the output of controllable distributed power is its expected value. The cross-limit probability of partial node voltage obtained by the two algorithms and the static unsafe probability of the system and the time taken are shown in Table 1. The calculation time of the semi-invariant method is until the cumulative distribution function of the state variable is generated, and the time of the Monte Carlo method is until the result of the state variable is obtained 6000 times, and the Monte Carlo results are the average of the results of 10 calculations. The cumulative distribution curves of active and reactive power of some branches are shown in Figure 3 and Figure 4.

It can be seen from Table 1 and Figure 3 and 4 that the random power flow based on the semi-invariant method can not only greatly improve the calculation efficiency, but also has high accuracy, and has high practical value in the calculation of random power flow.

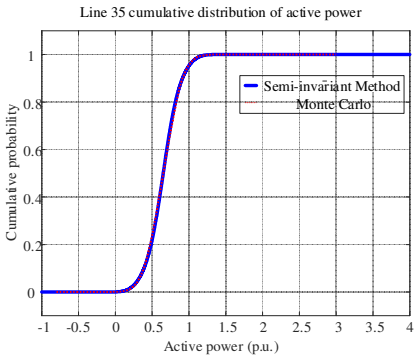

Figure 3. Comparison diagram of active power cumulative distribution curve of line 35

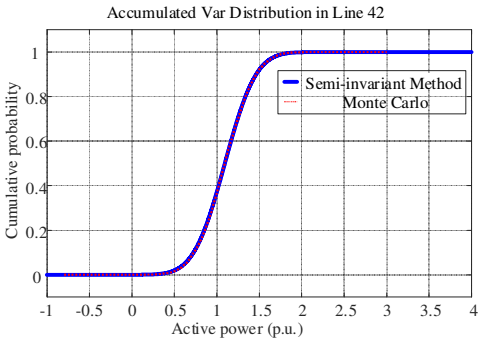

Figure 4. Comparison diagram of line 42 reactive power cumulative distribution curve

Table 1: Comparison of the results of the two algorithms

static unsafe probability	node 45	node 46	node 50	node 54	system	time/s
Monte Carlo Method	0.0008	0.5380	0.9624	0.9762	1	1.2858
Semi-invariant method	0.0005	0.5365	0.9608	0.9735	1	70.8865

In order to compare the impact of distributed power sources on the distribution network, it is divided into three situations for comparison.

Scenario 1: Considering only gas turbine (MT), its output is divided into three situations: 20 nodes output 200kW, 20 nodes output 400kW, 20 and 43 nodes each output 400kW;

Scenario 2: Consider gas turbines and electric vehicles (EV). Their output is similar to scenario 1. First, the output of 12 nodes is 200kW;

Scenario 3: Considering gas turbines, electric vehicles and photovoltaic power generation (PV), first connect 46-node photovoltaic modules with a rated maximum output of 200kW.

Since the lowest point of the system voltage is at node 54, analyze the probability of voltage overrun at node 54 to determine the impact on system reliability.

Table 2: DG's influence on the original system

	MT/MW	EV/MW	PV/MW	Node 54 static unsafe probability	network loss /kW	purchase cost/k$
Scenario 1	0.2	0	0	0.9923	0.2109	1.3624
	0.4			0.9902	0.1994	1.4551
	0.8			0.9819	0.1804	1.6417
Scenario 2	0.8	0.2	0	0.9851	0.1882	1.7073
		0.4		0.9878	0.1975	1.7734
		0.8		0.9880	0.1981	1.8997
Scenario 2	0.8	0.8	0.2	0.9823	0.1884	1.8651
			0.4	0.9736	0.1792	1.8307
			0.8	0.9735	0.1791	1.7675

It can be seen from the table that when the system is in the original structure, as the output of distributed power sources increases, the over-limit probability of the system nodes gradually decreases, the node voltage increases, and the system network loss gradually decreases. And as the power of electric vehicles connected to the grid gradually increases, the probability of exceeding the limit of the system node voltage increases, the insecurity of the system increases, and the network loss also increases. It can be concluded that the addition of gas turbines and photovoltaics can effectively improve the economy and reliability of the system, while the access of electric vehicles will reduce the economy and reliability of the system.

6.2 Optimization result analysis

First, reconstruct the original network. At this time, no distributed power supply is added to the network, and the disconnected branch is [69 70 14 50 47]. Under this network structure, the influence of the access of distributed power sources on the distribution system

is analyzed. The analysis method in section 4.1 is the same, and the results obtained are shown in Table 3.

Table 3: DG's influence on the refactored system

	MT/MW	EV/MW	PV/MW	Node 54 static unsafe probability	network loss /kW	purchase cost/k$
Scenario 1	0.2	0	0	0.9345	0.0942	1.3256
	0.4			0.9345	0.0894	1.4204
	0.8			0.9336	0.0866	1.6121
Scenario 2	0.8	0.2	0	0.9340	0.0896	1.6762
		0.4		0.9343	0.0940	1.7407
		0.8		0.9349	0.0943	1.8670
Scenario 3	0.8	0.8	0.2	0.9347	0.0938	1.8353
			0.4	0.9346	0.0937	1.8037
			0.8	0.9342	0.0935	1.7405

Comparing Table 2 and Table 3, it can be found that for the reconstructed distribution network, the static insecurity probability, network loss and power purchase cost of the system are all reduced. Different from the analysis results of the original network structure, as the output of gas turbines and photovoltaic power generation increases, the static insecure probability of the system and the reduction of the network loss are significantly smaller, or even unchanged. It shows that the network topology result after reconfiguration is relatively stable compared with that before reconfiguration, and the addition of distributed power sources will not have a significant impact on the network flow.

The particle swarm optimization algorithm based on stochastic power flow is used for calculation, and the Pareto "non-dominated" solution set is obtained, and then select the Pareto solution set. Due to the constraint relationship between the objective functions, when the power purchase cost is low, the static insecure probability often does not meet the system static security requirements. For power distribution systems, the safety of the system is more important. And from the above analysis, it can be seen that the static unsafe probability of the system is greater than 0.5, which is in a relatively unsafe state. Therefore, the coefficients of the selection mechanism a=0.2, b=0.6, c=0.2 are set to obtain the optimal solution.

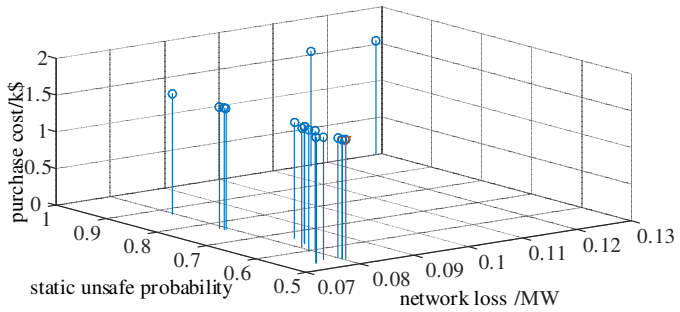

Figure 5. Distribution of optimal solution set

Compare the partial results of the optimal solution set with the original solution, as shown in Table 4. It can be clearly found from Table 4 that although the original network purchase cost is low, the static insecurity probability obviously does not meet the requirements, and the power quality is poor.

The reconfiguration solution in Table 4 is a reconfiguration scheme when the output of DG1 and DG2 is set to a definite value (200kW and 150kW, respectively). At this point, the optimal output of the algorithm depends on the output of DG1 and DG2, and only represents a solution in the set of comprehensive optimizations. Compared with the final solution of the optimization, although the cost of purchasing power is higher, the network loss is reduced. It can improve the probability of static insecurity and so on.

Table 4: Results comparison of partial optimal solution set

scheme	outage line	energy from DG1/kW	energy from DG2 /kW	network loss /kW	static insecurity probability	purchase cost/k$
Original network	69 70 71 72 73	0	0	0.2304	1	1.3985
optimal solution 1	69 14 12 50 42	0.1500	0.3368	0.0827	0.6321	1.5863
optimal solution 2	69 19 12 50 42	0.2690	0.3607	0.0793	0.5956	1.6541
optimal solution 3	69 70 12 50 41	0.2623	0.3872	0.0778	0.5677	1.6631
optimal solution 4	69 70 14 50 41	0.1756	0.1824	0.0881	0.8741	1.5260
optimal solution 5	69 15 12 51 42	0.1643	0.1591	0.0952	0.9686	1.5115
final solution	69 70 12 50 42	0.1500	0.4000	0.0807	0.5365	1.6161
reconfiguration solution	10 70 12 50 42	0.4000	0.4000	0.0782	0.5353	1.7357

7. Conclusion

In this paper, a multi-objective comprehensive optimization method for distribution network based on probabilistic power flow calculation is proposed. It is found that the integration of DG can effectively reduce network loss and greatly reduce the static insecurity probability. Pareto multi-objective optimization can obtain multiple optimization solutions, which is convenient for operators to choose according to actual conditions. At the same time, this method, which combines the randomness of distributed generation, DG output and contact switch combination, has potential application value to ensure the static security and economy of distribution system.

Acknowledgment

This work was financially supported by the Science and Technology Program of State Grid Shandong Electric Power Company (520606180144).

References

[1] S. Su, Y. Hu, L. He, K. Yamashita & S. Wang, An assessment procedure of distribution network reliability considering photovoltaic power integration, *IEEE Access*, *7*(1), 60171-60185, 2019.

[2] M. Masera, E. F. Bompard, F. Profumo & N. Hadjsaid, Smart (Electricity) grids for smart cities: assessing roles and societal impacts, Proceedings of the IEEE, *106*(4), 613-625, 2018.

[3] R. A. Jabr, I. Džafić & I. Huseinagić, Real time optimal reconfiguration of multiphase active distribution networks, *IEEE Transactions on Smart Grid*, *9*(6), 6829-6839, 2018.

[4] Ji, X.Q., Liu, Q., Yu & Y.J., Distribution network reconfiguration based on vector shift operation, *IET Generation, Transmission & Distribution*, *12*(13):3339-3345, 2018.

[5] A. R. Abbasi, Investigation of simultaneous effect of demand response and load uncertainty on distribution feeder reconfiguration, *IET Generation, Transmission & Distribution*, *14*(8), 1438-1449, 2019..

[6] Y. Liu, J. Li & L. Wu, Coordinated optimal network reconfiguration and voltage regulator/DER control for unbalanced distribution systems, *IEEE Transactions on Smart Grid*, *10*(3), 2912-2922, 2019.

[7] H. Wu, P. Dong & M. Liu, Distribution network reconfiguration for loss reduction and voltage stability with random fuzzy uncertainties of renewable energy generation and load, *IEEE Transactions on Industrial Informatics*, *16*(9), 5655-5666, 2020.

[8] H. Wang, W. Zhang & Y. Liu, A robust measurement placement method for active distribution system state estimation considering network reconfiguration, *IEEE Transactions on Smart Grid*, *9*(3), 2108-2117, 2017.

[9] A. Kavousi-Fard & T. Niknam, Optimal distribution feeder reconfiguration for reliability improvement considering uncertainty, *IEEE Transactions on Power Delivery*, *29*(3), 1344-1353, 2014.

[10] Su, C.L., Probabilistic load-flow computation using point estimate method, *IEEE Transactions on Power Systems*, *20*(4): 1843-1851, 2015.

[11] Y. Z. Li & Q. H. Wu, Downside risk constrained probabilistic optimal power flow with wind power integrated, *IEEE Transactions on Power Systems*, *31*(2), 1649-1650, 2015.

[12] Behdad, A., Hooshmand, R. A, & Gholipour. E, Decreasing activity cost of a distribution system company by reconfiguration and power generation control of DGs based on shuffled frog leaping algorithm, *Electric Power Systems Research*, *61*(10): 48-55, 2016.

[13] Z. Wang, C. Shen, F. Liu & F. Gao, Analytical expressions for joint distributions in probabilistic load flow, *IEEE Transactions on Power Systems*, *32*(3), 2473-2474,2016.

[14] Z. Liu, Y. Liu, G. Qu, X. Wang & X. Wang, Intra-day dynamic network reconfiguration Based on probability analysis considering the deployment of remote control switches, *IEEE Access*, *7*(1), 145272-145281, 2019.

[15] H. Haghighat & B. Zeng, Distribution system reconfiguration under uncertain load and renewable Generation, *IEEE Transactions on Power Systems*, *31*(4), 2666-2675, 2016.

[16] Eldurssi, A.M., O'Connell & R.M, A fast non-dominated sorting guided genetic algorithm for multi-objective power distribution system reconfiguration problem, *IEEE Transactions on Power Systems, 30*(2): 593-601, 2017.

[17] Andervazh, M.R., Olamaei, J., Haghifam & M.R, Adaptive multi-objective distribution network reconfiguration using multi-objective discrete particles swarm optimization algorithm and graph theory, *IET Generation, Transmission and Distribution, 7* (12): 1367-1382 , 2016.

[18] X. Chen, W. Wu & B. Zhang, Robust capacity assessment of distributed generation in unbalanced distribution networks incorporating ANM techniques, *IEEE Transactions on Sustainable Energy*, *9*(2), 651-663, 2017.

[19] Y. Fu & H. Chiang, Toward optimal multiperiod network reconfiguration for increasing the hosting capacity of distribution networks, *IEEE Transactions on Power Delivery*, *33*(5), 2294-2304, 2018.

[20] Goswami, S. K., Basu & S. K, A new algorithm for the reconfiguration of distribution feeders for loss minimization, *IEEE Transactions on Power Delivery*, *7*(3): 1484-1491, 1992.